Exact Calculation of the Uncertainty on the Input Reflection Coefficient of Arbitrary Two Ports Due to Mismatches and Arbitrary Reference Planes

HERMAN TROMP

Abstract—**A specific problem of worst case analysis of microwave networks is dealt with. Exact formulas are derived for the upper and lower limits of the amplitude of the input reflection coefficient of an arbitrary two port, in the presence of mismatched source and load and/or arbitrary reference planes. The derivation is based on certain properties of the bilinear transformation.**

I. Introduction

IT WAS SHOWN by Bandler, Liu, and Tromp [1] that, in the worst case analysis of microwave two ports, the effect of a mismatched source and load should not be neglected, as compared with the effect of physical tolerances and model uncertainties. Explicit formulas were derived for the extrema of the modulus of the input reflection coefficient of a lossless two port, referred to real normalization impedances, under various conditions of source and load mismatches. In this paper, we shall generalize those formulas.

We will consider the situation depicted in Fig. 1. The S-matrix of the two port is referred to Z_1' and Z_2'. Source and load impedances Z_S and Z_L are represented by their reflection coefficients ρ_S and ρ_L with respect to Z_1 and Z_2, respectively. Z_i and Z_i' $(i=1,2)$ may be complex. Let

$$\rho_S=|\rho_S|e^{j\phi_S}, \quad \rho_L=|\rho_L|e^{j\phi_L}. \tag{1}$$

We assume that ϕ_S and ϕ_L can vary between 0 and 2π and that $|\rho_S|$ and $|\rho_L|$ are either given or limited by

$$0\leqslant|\rho_S|\leqslant|\rho_S|^+, \quad 0\leqslant|\rho_L|\leqslant|\rho_L|^+. \tag{2}$$

This corresponds to the realistic situation, where only a VSWR or a maximal VSWR is specified for source and load. We are interested in the input reflection coefficient

$$\rho_{\text{in}}=\frac{Z_{\text{in}}-Z_S^*}{Z_{\text{in}}+Z_S} \tag{3}$$

and we shall derive expressions for the extrema of $|\rho_{\text{in}}|$, i.e.,

Manuscript received May 29, 1978; revised September 8, 1978. This paper is based on material presented at the 1978 IEEE-MTT-S International Microwave Symposium, Ottawa, Canada, June 27–29, 1978. The work was supported by a grant of the Belgian NFWO (National Research Fund).

The author is with the Laboratory of Electromagnetism and Acoustics, Univeristy of Ghent, Ghent, Belgium.

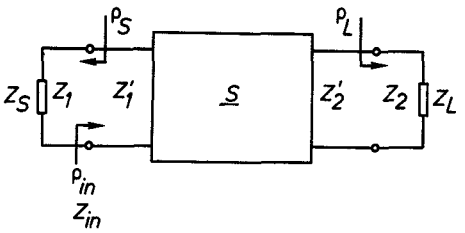

Fig. 1. Two port with mismatched source and load.

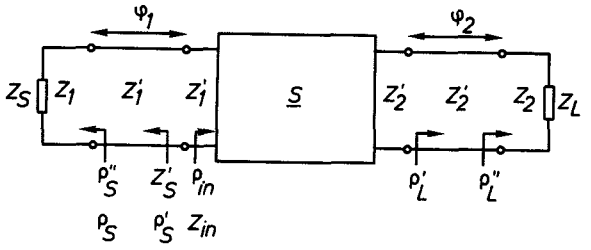

Fig. 2. Two port with arbitrary reference planes.

$$|\rho_{\text{in}}|_M=\operatorname*{Max}_{\phi_S,\phi_L}|\rho_{\text{in}}|, \quad |\rho_{\text{in}}|_m=\operatorname*{Min}_{\phi_S,\phi_L}|\rho_{\text{in}}| \tag{4}$$

or, alternatively,

$$|\rho_{\text{in}}|^+=\operatorname*{Max}_{|\rho_S|,|\rho_L|,\phi_S,\phi_L}|\rho_{\text{in}}|, |\rho_{\text{in}}|^-=\operatorname*{Min}_{|\rho_S|,|\rho_L|,\phi_S,\phi_L}|\rho_{\text{in}}|. \tag{5}$$

Another situation which shall be dealt with is shown in Fig. 2, where the lengths of the connecting lines at input and output (given by phase angles ϕ_1 and ϕ_2) are also arbitrary. We shall consider only real Z_i, Z_i' $(i=1,2)$ in this case. The extrema in (4) and (5) will be taken over ϕ_1 and ϕ_2, too. Both completely arbitrary positions of the reference planes and positions affected by a given uncertainty will be considered.

The expressions to be derived are useful for worst case analysis and fit into the general formulation of the tolerance problem as given by Tromp [2], [3]. This means that a tolerance optimization procedure, as described by Bandler *et al.* [1], [4], [5] and Pinel and Roberts [6], can lead to a compromise between the tolerances within the network (i.e., its cost) and the quality of source and load. To a certain extent the results, especially for the case of Fig. 2,

0018-9480/78/1200-0973$00.75 ©1978 IEEE

can be used to design a subnetwork of a large network separately, allowing for an uncertainty on the subnetworks, connected to it, and on the length of the connecting lines. Our derivation [3] will be based on certain properties of the complex bilinear transformation.

II. Bilinear Transformations

Consider the transformation (w,z,a,b,c,d complex)

$$w=\frac{az+b}{cz+d} \tag{6}$$

which is known to transform circles into circles. Without loss of generality, we can consider

$$w=\mathrm{Re}^{j\phi}, \qquad 0\leqslant\phi\leqslant 2\pi \tag{7}$$

as a circle in the w plane. The corresponding circle in the z plane (Fig. 3) is described by

$$z=z_0+re^{j\theta}, \qquad 0\leqslant\theta\leqslant 2\pi \tag{8}$$

with

$$z_0=\frac{R^2c^*d-a^*b}{|a|^2-R^2|c|^2}, \quad r=\frac{R|ad-bc|}{||a|^2-R^2|c|^2|} \tag{9}$$

as its center and radius, respectively.

The extrema of $|z|$ for $0\leqslant\phi\leqslant 2\pi$ are determined by the points (see Fig. 3)

$$z_M=z_0\left(1+\frac{r}{|z_0|}\right) \tag{10}$$

$$z_m=z_0\left(1-\frac{r}{|z_0|}\right) \tag{11}$$

and are given by

$$|z_M|=\operatorname*{Max}_{\phi}|z|=|z_0|+r \tag{12}$$

$$|z_m|=\operatorname*{Min}_{\phi}|z|=||z_0|-r|. \tag{13}$$

The corresponding points in the w plane are found substituting (10) and (11) into (6). One can prove that $|z_M|$ and $|z_m|$, as functions of R, behave as shown in Table I. Typical curves are given in Fig. 4. If we now let R vary according to

$$R^-\leqslant R\leqslant R^+ \tag{14}$$

then the extrema of $|z|$ over all ϕ and all R are

$$|z|^+=\operatorname*{Max}_{\phi,R}|z|=\begin{cases}|z_M(R^+)|, & \text{if } R^+<\left|\dfrac{a}{c}\right| \\ \infty, & \text{if } R^-\leqslant\left|\dfrac{a}{c}\right|\leqslant R^+ \\ |z_M(R^-)|, & \text{if } R^->\left|\dfrac{a}{c}\right|\end{cases} \tag{15}$$

$$|z|^-=\operatorname*{Min}_{\phi,R}|z|=\begin{cases}|z_m(R^+)|, & \text{if } R^+<\left|\dfrac{b}{d}\right| \\ 0, & \text{if } R^-\leqslant\left|\dfrac{b}{d}\right|\leqslant R^+ \\ |z_m(R^-)|, & \text{if } R^->\left|\dfrac{b}{d}\right|\end{cases} \tag{16}$$

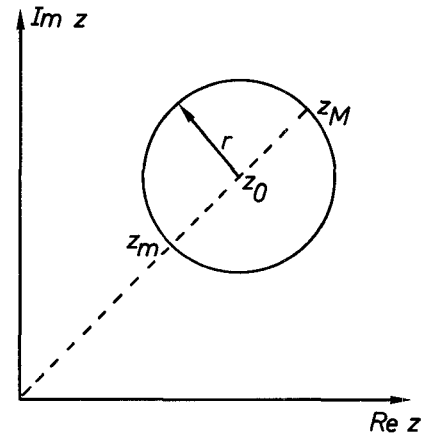

Fig. 3. Transformed circle in the z plane.

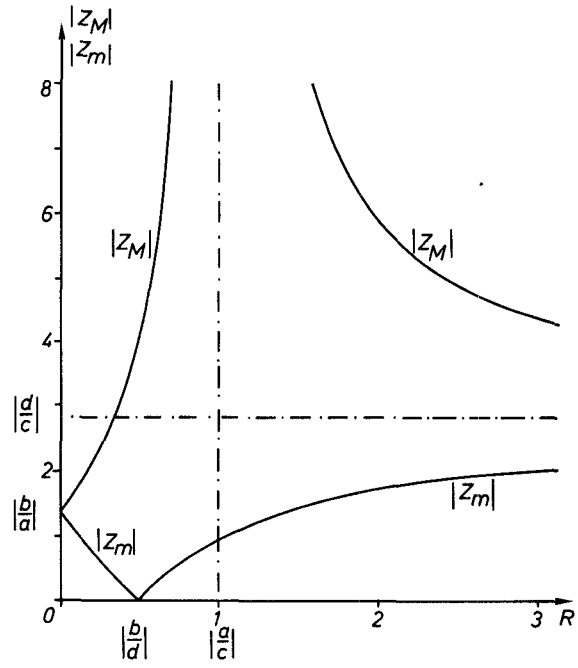

Fig. 4. Bilinear transformation: limits of $|z|$ (typical).

TABLE I
Behavior of $x|z_M(R)|$ and $|z_m(R)|$

Case $\left\|\frac{b}{a}\right\| < \left\|\frac{d}{c}\right\|$							
R	0		$\left\|\frac{b}{d}\right\|$		$\left\\|\frac{a}{c}\right\\|$		∞
$\|z_M\|$	$\left\|\frac{b}{a}\right\|$	↗	↗	↗	∞	↘	$\left\|\frac{d}{c}\right\|$
$\|z_m\|$	$\left\|\frac{b}{a}\right\|$	↘	0	↗	↗	↗	$\left\|\frac{d}{c}\right\|$
Case $\left\|\frac{b}{a}\right\| > \left\|\frac{d}{c}\right\|$							
R	0		$\left\\|\frac{a}{c}\right\\|$		$\left\|\frac{b}{d}\right\|$		∞
$\|z_M\|$	$\left\|\frac{b}{a}\right\|$	↗	∞	↘	↘	↘	$\left\|\frac{d}{c}\right\|$
$\|z_m\|$	$\left\|\frac{b}{a}\right\|$	↘	↘	↘	0	↗	$\left\|\frac{d}{c}\right\|$

TABLE II
z_M AND z_m WHEN $\arg a+\arg d=\arg b+\arg c$

	Case $\left\|\frac{b}{a}\right\| < \left\|\frac{d}{c}\right\|$		Case $\left\|\frac{b}{a}\right\| > \left\|\frac{d}{c}\right\|$	
	$R < R_0$	$R > R_0$	$R < R_0$	$R > R_0$
z_M	z_B	z_A	z_A	z_B
z_m	z_A	z_B	z_B	z_A

The following special case of the general expressions (12) and (13) is of interest: if

$$\arg a+\arg d=\arg b+\arg c \tag{17}$$

then the values of $|z_M|$ and $|z_m|$ are given by Table II, where

$$|z_A|=\left|\frac{|b|-R|d|}{|a|-R|c|}\right| \tag{18}$$

$$|z_B|=\left|\frac{|b|+R|d|}{|a|+R|c|}\right| \tag{19}$$

and

$$R_0=\sqrt{\left|\frac{ab}{cd}\right|}\,. \tag{20}$$

Consider now the transformation

$$z=\frac{w^*d^*-b^*}{a-wc} \tag{21}$$

which does not transform circles into circles [3], but yields the same $|z|$ as (6). This means that all results, (12)–(20), also apply for (21), which we therefore call the pseudobilinear transformation.

The results of this section can be applied to a number of problems in microwave network theory, such as the worst case analysis problems of Section I.

III. Effect of Mismatches

In Fig. 1, we have

$$|\rho_{\text{in}}|=\left|\frac{\rho-\rho_S^*}{1-\rho\rho_S}\right| \tag{22}$$

where ρ is the input reflection coefficient with respect to Z_1^*, i.e.,

$$\rho=\frac{Z_{\text{in}}-Z_1}{Z_{\text{in}}+Z_1^*}\,. \tag{23}$$

Equation (22) represents a pseudobilinear transformation. The results of Section II can be used to find the extrema of $|\rho_{\text{in}}|$, for all possible ρ_S and for a given ρ. Special case (17) applies here. From (18) and (19), it is clear that the extrema of $|\rho_{\text{in}}|$ are a function of $|\rho|$ only.

ρ depends only on ρ_L and $|\rho|$ can be extremized over all possible ρ_L, independently of ρ_S. As a result of this, the effects of the variations of the source and load on the input reflection coefficient can be separated. It turns out that this is not possible for the effect on the insertion loss.

We have

$$\rho_L=\frac{a\rho+b}{c\rho+d} \tag{24}$$

with

$$\begin{aligned}
a&=(1+S'_{11}\Delta_1)(1+S'_{22}\Delta_2)-S'_{12}S'_{21}\Delta_1\Delta_2\\
b&=-(\Delta_1^*+S'_{11})(1+S'_{22}\Delta_2)+S'_{12}S'_{21}\Delta_2\\
c&=(1+S'_{11}\Delta_1)(\Delta_2^*+S'_{22})-S'_{12}S'_{21}\Delta_1\\
d&=-(\Delta_1^*+S'_{11})(\Delta_2^*+S'_{22})+S'_{12}S'_{21}\\
S'_{11}&=\gamma_1^*S_{11},\quad S'_{22}=\gamma_2^*S_{22},\quad S'_{12}S'_{21}=\gamma_1^*\gamma_2^*S_{12}S_{21}\\
\gamma_i&=\frac{Z_i'^*+Z_i^*}{Z_i'+Z_i},\quad \Delta_i=\frac{Z_i'-Z_i^*}{Z_i'+Z_i},\qquad i=1,2.
\end{aligned} \tag{25}$$

Equation (24) is a bilinear transformation. The limits $|\rho_M|$ and $|\rho_m|$ of $|\rho|$ over all ϕ_L can be found from (12) and (13), and the limits $|\rho|^+$ and $|\rho|^-$ over all ϕ_L and all $|\rho_L|$ from (15) and (16) (with $R^-=0$, $R^+=|\rho_L|^+$). The combination of these extrema with those derived from (22) yields exact expressions for the extrema of $|\rho_{\text{in}}|$. We find

$$|\rho_{\text{in}}|_M=\begin{cases}
K^+(|\rho_M|,|\rho_S|), & \text{if } |\rho_M|<1\leqslant\dfrac{1}{|\rho_S|}\\
K^-(|\rho_M|,|\rho_S|), & \text{if } |\rho_M|<\dfrac{1}{|\rho_S|}\leqslant 1\\
& \text{or if } 1\leqslant|\rho_M|<\dfrac{1}{|\rho_S|}\\
K^+(|\rho_m|,|\rho_S|), & \text{if } \dfrac{1}{|\rho_S|}\leqslant 1<|\rho_m|\\
K^-(|\rho_m|,|\rho_S|), & \text{if } \dfrac{1}{|\rho_S|}<|\rho_m|\leqslant 1\\
& \text{or if } 1\leqslant\dfrac{1}{|\rho_S|}<|\rho_m|\\
\infty, & \text{if } |\rho_m|\leqslant\dfrac{1}{|\rho_S|}\leqslant|\rho_M|
\end{cases} \tag{26}$$

$$|\rho_{\text{in}}|_m=\begin{cases}
K^-(|\rho_M|,|\rho_S|), & \text{if } |\rho_M|<|\rho_S|\leqslant 1\\
& \text{or if } 1\leqslant|\rho_M|<|\rho_S|\\
K^+(|\rho_M|,|\rho_S|), & \text{if } |\rho_M|<1\leqslant|\rho_S|\\
K^-(|\rho_m|,|\rho_S|), & \text{if } |\rho_S|<|\rho_m|\leqslant 1\\
& \text{or if } 1\leqslant|\rho_S|<|\rho_m|\\
K^+(|\rho_m|,|\rho_S|), & \text{if } |\rho_S|\leqslant 1<|\rho_m|\\
0, & \text{if } |\rho_m|\leqslant|\rho_S|\leqslant|\rho_M|
\end{cases} \tag{27}$$

with the functions

$$K^+(x_1,x_2)=\left|\frac{x_1+x_2}{1+x_1x_2}\right| \tag{28}$$

$$K^-(x_1,x_2)=\left|\frac{x_1-x_2}{1-x_1x_2}\right|=K^+(x_1,-x_2). \tag{29}$$

We also find

$$|\rho_{in}|^+ = \begin{cases} K^+(|\rho|^+, |\rho_S|^+), \\ \quad \text{if } |\rho_L|^+ < \left|\frac{a}{c}\right| \text{ and } |\rho|^+ < 1 \leqslant \frac{1}{|\rho_S|^+} \\ K^-(|\rho|^+, |\rho_S|^+), \\ \quad \text{if } |\rho_L|^+ < \left|\frac{a}{c}\right| \text{ and} \\ \quad \text{either } |\rho|^+ < \frac{1}{|\rho_S|^+} \leqslant 1 \\ \quad \text{or } 1 \leqslant |\rho|^+ < \frac{1}{|\rho_S|^+} \\ \infty, \\ \quad \text{if } |\rho_L|^+ \geqslant \left|\frac{a}{c}\right| \text{ or } |\rho|^+ \geqslant \frac{1}{|\rho_S|^+} \end{cases} \tag{30}$$

$$|\rho_{in}|^- = \begin{cases} K^-(|\rho|^-, |\rho_S|^+), \\ \quad \text{if } |\rho_L|^+ < \left|\frac{b}{d}\right| \text{ and} \\ \quad \text{either } 1 \leqslant |\rho_S|^+ < |\rho|^- \\ \quad \text{or } |\rho_S|^+ < |\rho|^- \leqslant 1 \\ K^+(|\rho|^-, |\rho_S|^+), \\ \quad \text{if } |\rho_L|^+ < \left|\frac{b}{d}\right| \text{ and } |\rho_S|^+ \leqslant 1 < |\rho|^- \\ 0, \\ \quad \text{if } |\rho_L|^+ \geqslant \left|\frac{b}{d}\right| \text{ or } |\rho|^- \leqslant |\rho_S|^+ \end{cases} \tag{31}$$

In many practical situations, (26), (27), (30), and (31) can be simplified considerably, e.g., when Z_S and Z_L are passive.

IV. Indefinite Reference Planes

Consider Fig. 2, with Z_i and Z_i' $(i=1,2)$ real. Assume that besides ϕ_S, ϕ_L, $|\rho_S|$, and $|\rho_L|$, also ϕ_1 and ϕ_2 are variable according to

$$\phi_i^- \leqslant \phi_i \leqslant \phi_i^+, \qquad i=1,2. \tag{32}$$

Now let ρ_S' be the reflection coefficient of Z_S' with respect to Z_1' and ρ_S'' that of Z_S with respect to Z_1' (see Fig. 2). Then

$$\rho_S' = \rho_S'' e^{-2j\phi_1} \tag{33}$$

and

$$\rho_S = \frac{\rho_S'' + \Delta_1}{1 + \rho_S'' \Delta_1}. \tag{34}$$

Equation (34) represents again special case (17) of the bilinear transformation. According to the theory of Section II, the region in the complex plane, within which ρ_S'' can vary, due to the variations of ρ_S, is circular. The region of all possible ρ_S' follows then immediately from (32) and (33). The two cases of interest are indicated in Fig. 5. In particular, the extrema $|\rho_S'|^-$ and $|\rho_S'|^+$ of $|\rho_S'| = |\rho_S''|$, over all possible ρ_S, can be obtained from Table II. The same can be done at the load.

If the reference planes are completely arbitrary, then

$$\phi_i^+ - \phi_i^- \geqslant \pi, \qquad i=1,2. \tag{35}$$

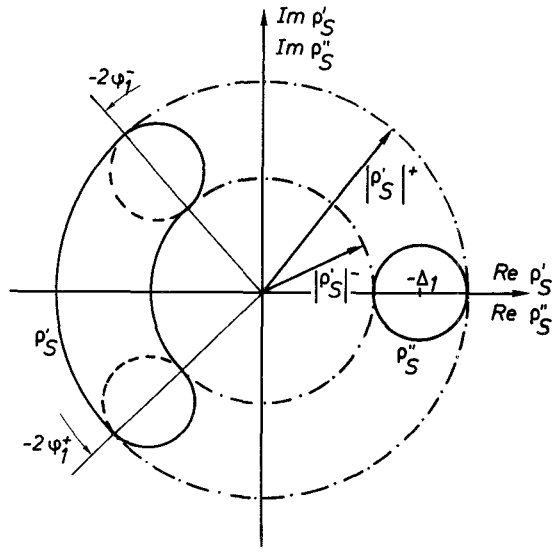

Fig. 5. Indefinite reference planes; possible regions for ρ_S'' and ρ_S' (—·—· if $\phi_1^+ - \phi_1^- \geqslant \pi$), (——if $\phi_1^+ - \phi_1^- < \pi$).

We arrive at a situation similar to that of Fig. 1, where the moduli of the source and load reflection coefficients (*in casu* ρ_S' and ρ_L') can now vary between (nonzero) lower and upper limits and where their phases are completely arbitrary. The derivation of Section III can be repeated, now using $R^- \neq 0$ in (15) and (16). The resulting formulas for the extrema of $|\rho_{in}|$ become rather complicated but can easily be implemented in a computer program.

If the reference planes are affected by an uncertainty, but not completely arbitrary, i.e., if, for any i, $\phi_i^+ - \phi_i^- < \pi$, the extrema of $|\rho_{in}|$ can be calculated as follows.

1) Assume (35); calculate the extrema of $|\rho_{in}|$, as indicated above, as well as the ρ_S' and ρ_L' yielding those extrema, by appropriate substitution of (10) and (11) in (6).

2) If both ρ_S' and ρ_L' are within their possible region (see Fig. 5), the extrema calculated in 1) are the true limits of $|\rho_{in}|$.

3) If either ρ_S' or ρ_L' is outside its possible region, take for the corresponding ϕ_i alternatively ϕ_i^- and ϕ_i^+, and solve the resulting extremum problems. This implies either a situation where both ϕ_1 and ϕ_2 are fixed, for which the formulas of Section III apply, or a situation where one ϕ_i is fixed and the other variable, according to (35), which is a special case of step 1). In the latter case, steps 2) and 3) have to be repeated eventually. As a result of this procedure, several extremum problems are solved. The true bounds of $|\rho_{in}|$ are finally found by inspection of the different solutions which correspond to possible ρ_S' and ρ_L'. Explicit formulas for the extrema of $|\rho_{in}|$ are not available in this case, but the procedure can be implemented in a computer program in a straightforward way.

V. Lossless Two Ports

If $Z_i = Z_i'$ $(i=1,2)$ are real and if the two port is lossless, (24) is also reduced to special case (17). The resulting formulas become simpler. We find

$$|\rho_{\text{in}}|_M = \begin{cases} K^+(|S_{22}|, K_p), & \text{if } K_p \leqslant 1 \\ K^-(|S_{22}|, K_q), & \text{if } K_p > 1 \text{ and } K_q < \dfrac{1}{|S_{22}|} \\ K^-(|S_{22}|, K_p), & \text{if } K_p > \dfrac{1}{|S_{22}|} \\ \infty, & \text{if } 1 < K_p \leqslant \dfrac{1}{|S_{22}|} \leqslant K_q \end{cases} \tag{36}$$

$$|\rho_{\text{in}}|_m = \begin{cases} K^+(|S_{22}|, K_p), & \text{if } K_p \geqslant 1 \\ K^-(|S_{22}|, K_p), & \text{if } K_p < |S_{22}| \\ K^-(|S_{22}|, K_q), & \text{if } K_p < 1 \text{ and } K_q > |S_{22}| \\ 0, & \text{if } K_q \leqslant |S_{22}| \leqslant K_p < 1 \end{cases} \tag{37}$$

with

$$K_p = K^+(|\rho_S|, |\rho_L|) \tag{38}$$

$$K_q = K^-(|\rho_S|, |\rho_L|) \tag{39}$$

and

$$|\rho_{\text{in}}|^+ = \begin{cases} K^+(|S_{22}|, K_p^+), & \text{if } |\rho_L|^+ \leqslant 1 \text{ and } |\rho_S|^+ \leqslant 1 \\ K^-(|S_{22}|, K_q^+), & \text{if } K_p^+ > 1, \quad |\rho_S|^+ |\rho_L|^+ < 1 \\ & \text{and } K_q^+ < \dfrac{1}{|S_{22}|} \\ \infty, & \text{in all other cases} \end{cases} \tag{40}$$

$$|\rho_{\text{in}}|^- = \begin{cases} K^-(|S_{22}|, K_p^+), & \text{if } K_p^+ < |S_{22}| \\ 0, & \text{if } K_p^+ \geqslant |S_{22}| \end{cases} \tag{41}$$

with K_p^+ and K_q^+ analogous to K_p and K_q. If Z_S and Z_L are passive, the formulas given in [1] are found.

VI. Example

As an example, we consider the transistor HP 35821E (bias $I_C = 15$ mA, $V_{CE} = 15$ V). Fig. 6 gives the limits of $|\rho_{\text{in}}|$, if $|\rho_S|^+ = |\rho_L|^+ = 0.2$, in two cases. $|\rho_{\text{in}}|_M$ and $|\rho_{\text{in}}|^+$ coincide, as well as $|\rho_{\text{in}}|_m$ and $|\rho_{\text{in}}|^-$. The result of a Monte–Carlo analysis, where ϕ_S, ϕ_L, $|\rho_S|$, and $|\rho_L|$ were varied at random in their intervals, is also indicated. One thousand sample points were used. If only ϕ_S and ϕ_L are assumed variable, the results of a Monte–Carlo analysis with 1000 sample points cannot be distinguished from the bounds calculated with our formulas. Fig. 7 illustrates the effect of arbitrary reference planes. Curves *a* correspond to reference planes fixed at a nominal position and curves *c* to completely arbitrary reference planes. For curves *b*, a given error on the position of the reference planes was assumed. In this case, both ϕ_1 and ϕ_2 should have one of their extreme values to yield the extrema of $|\rho_{\text{in}}|$.

VII. Conclusion

Explicit formulas and numerical procedures were derived for the calculation of the limits of the input reflection coefficient of an arbitrar two port, under various conditions of source and load. The example shows that even moderate mismatches or uncertainties on the position of the reference planes can have a considerable effect. They should be accounted for in any realistic design procedure.

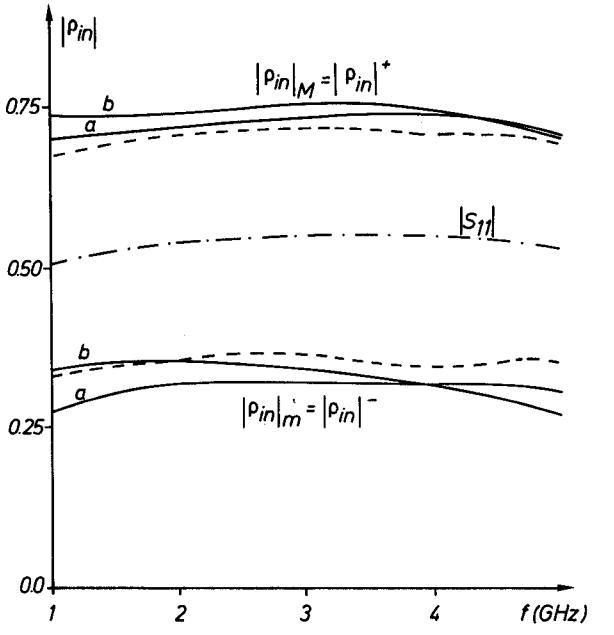

Fig. 6. Input reflection coefficient of 35821E, with $|\rho_S|^+ = |\rho_L|^+ = 0.2$. Curve *a*: $Z_i = Z_i' = 50$; curve *b*: $Z_1 = 50 + 0.5j$, $Z_2 = 49 - 2j$, $Z_1' = 45 + 5j$, $Z_2' = 55 - 7j$. (– –Monte-Carlo, case (a), 1000 sample points.)

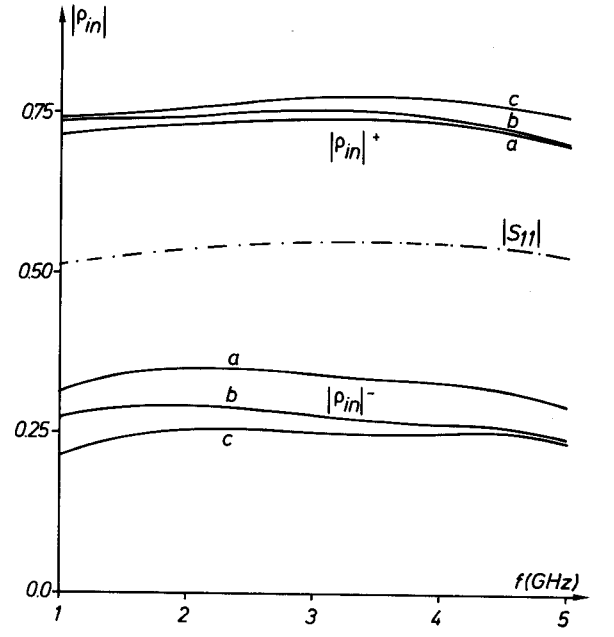

Fig. 7. Input reflection coefficient of 35821E, with $|\rho_S|^+ = |\rho_L|^+ = 0.2$, $Z_1 = 50$, $Z_1' = 45$, $Z_2 = 49$, $Z_2' = 55$. Curve *a*: fixed reference planes; curve *b*: indefinite reference planes, $10° \leqslant \phi_1, \leqslant 40°$ and $90° \leqslant \phi_2 \leqslant 150°$; and curve *c*: indefinite reference planes, $0° \leqslant \phi_1, \phi_2 \leqslant 360°$.

References

[1] J. W. Bandler, P. C. Liu, and H. Tromp, "Integrated approach to microwave design," *IEEE Trans. Microwave Theory Tech.*, vol. MTT-24, pp. 584–591, Sept. 1976.

[2] H. Tromp, "The generalized tolerance problem and worst case

search," *Proc. Conf. Computer Aided Design of Electronic, Microwave Circuits and Systems*, Hull, England, pp. 72–77, July 1977.
[3] ——, "Generalized worst case design, with applications to microwave networks" (in Dutch), Ph.D. dissertation, Faculty of Engineering, University of Ghent, Ghent, Belgium, May 1978.
[4] J. W. Bandler, P. C. Liu, and J. H. K. Chen, "Worst case network tolerance optimization," *IEEE Trans. Microwave Theory Tech.*, vol. MTT-23, pp. 630–641, Aug. 1975.
[5] J. W. Bandler, P. C. Liu, and H. Tromp, "A nonlinear programming approach to optimal design centering, tolerancing, and tuning," *IEEE Trans. Circuits Syst.*, vol. CAS-23, pp. 155–165, Mar. 1976.
[6] J. F. Pinel and K. A. Roberts, "Tolerance assignment in linear networks using nonlinear programming," *IEEE Trans. Circuit Theory*, vol. CT-19, pp. 475–479, Sept. 1972.

An Approximate Dynamic Spatial Green's Function for Microstriplines

Y. LEONARD CHOW, MEMBER, IEEE, AND IBRAHIM N. EL-BEHERY

***Abstract*—A dynamic model of both charge and current images is constructed to give rise to a frequency-dependent dyadic Green's function in the space domain for microstriplines. While the spatial Green's function is approximate, its image model is very simple, and the propagation constants calculated from it agree well with published results.**

I. Introduction

THE DYADIC Green's function in the spectral domain for microstriplines has been derived by Denlinger [1]. The expression of this Green's function, however, while being exact, is quite complicated making its use difficult in arbitrarily shaped structures.

The dyadic Green's function in the space domain, on the other hand, may overcome this difficulty, but it is generally not known in a closed form. A static equivalent, however, has been derived by Silvester [2] from a model of charge images. The simplicity of this model and the good physical insight it gives naturally suggest the possibility of its extension to a dynamic model that can reasonably approximate the dyadic Green's function at the higher frequencies.

While such an approach may be used to construct dynamic Green's functions in three dimensions for arbitrarily shaped microstrip structures, this paper, being a first attempt in this direction, considers only the extension to the Green's function in two dimensions for microstriplines.

In this paper the two-dimensional Green's function is defined as the kernel function of the integral equation

Manuscript received May 29, 1978; revised July 28, 1978. This work was supported in part by the Communications Research Center of Canada through the Department of Supply and Services under Contract 08SU. 36100-7-9511 and in part by the National Research Council of Canada under Grant A3804.

The authors are with the Department of Electrical Engineering, University of Waterloo, Waterloo, Ont. N2L 3G1, Canada.

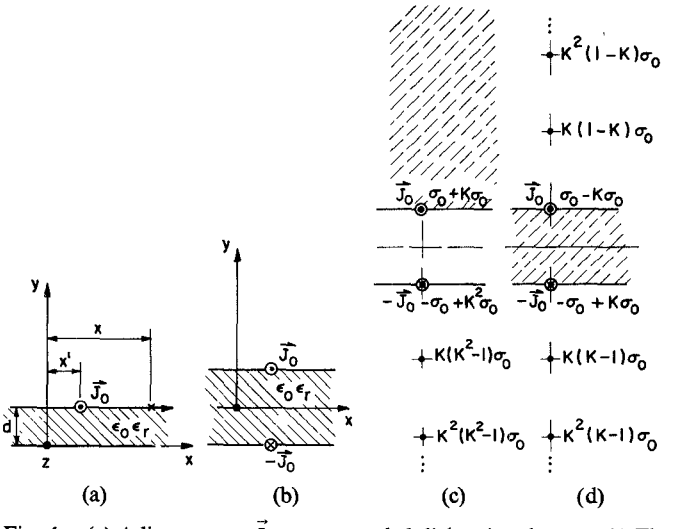

Fig. 1. (a) A line current $\vec{J}_0$ on a grounded dielectric substrate. (b) The equivalent of (a): a dielectric substrate with two true currents. (c) The model for the outside (dashed) region with true currents and charges $\pm\vec{J}_0$ and $\pm\sigma_0$ and image charges σ_n. The magnitudes of the images are indicated with $K=(1-\epsilon_r)/(1+\epsilon_r)$. The separation between adjacent images is $2d$. (d) The model for the inside (dashed) region.

$$\vec{E}_{\tan}(x)=\int \bar{\bar{G}}(x,x')\cdot\vec{J}_0(x')dx' \tag{1}$$

where, according to the geometry of Fig. 1(a),

$$\bar{\bar{G}}(x,x')=\begin{bmatrix} G_{xx}(x,x') & G_{xz}(x,x') \\ G_{zx}(x,x') & G_{zz}(x,x') \end{bmatrix} \tag{2}$$

and where $\vec{J}_0(x)$ and $\vec{E}_{\tan}(x)$ are, respectively, the density of the current vector and the tangential electric field vector on the surface of the grounded dielectric substrate of Fig. 1(a).

0018-9480/78/1200-0978$00.75 ©1978 IEEE